

# UC Irvine

## UC Irvine Previously Published Works

### Title

Beam ion losses due to energetic particle geodesic acoustic modes

### Permalink

<https://escholarship.org/uc/item/6vp3k29n>

### Journal

Nuclear Fusion, 52(12)

### ISSN

0029-5515

### Authors

Fisher, RK  
Pace, DC  
Kramer, GJ  
[et al.](#)

### Publication Date

2012-12-01

### DOI

10.1088/0029-5515/52/12/123015

### Copyright Information

This work is made available under the terms of a Creative Commons Attribution License, available at <https://creativecommons.org/licenses/by/4.0/>

Peer reviewed

# Beam ion losses due to energetic particle geodesic acoustic modes

R.K. Fisher<sup>1</sup>, D.C. Pace<sup>1</sup>, G.J. Kramer<sup>2</sup>, M.A. Van Zeeland<sup>1</sup>,  
R. Nazikian<sup>2</sup>, W.W. Heidbrink<sup>3</sup> and M. García-Muñoz<sup>4</sup>

<sup>1</sup> General Atomics, PO Box 85608, San Diego, CA 92186-9784, USA

<sup>2</sup> Princeton Plasma Physics Laboratory, PO Box 451, Princeton, NJ 08543-0451, USA

<sup>3</sup> University of California-Irvine, Irvine, CA 92697, USA

<sup>4</sup> Max Planck-Institut für Plasmaphysik, Garching, Germany

Received 24 May 2012, accepted for publication 31 October 2012

Published 20 November 2012

Online at [stacks.iop.org/NF/52/123015](http://stacks.iop.org/NF/52/123015)

## Abstract

We report the first experimental observations of fast-ion loss in a tokamak due to energetic particle driven geodesic acoustic modes (EGAMs). A fast-ion loss detector installed on the DIII-D tokamak observes bursts of beam ion losses coherent with the EGAM frequency. The EGAM activity results in a significant loss of beam ions, comparable to the first orbit losses. The pitch angles and energies of the measured fast-ion losses agree with predictions from a full orbit simulation code SPIRAL, which includes scattering and slowing-down.

(Some figures may appear in colour only in the online journal)

## 1. Introduction

Fast ions from neutral beam injection, ion cyclotron heating, and fusion reactions play a fundamental role in the heating and stability of tokamak plasmas. Large fast-ion densities can drive collective instabilities, which in turn degrade fast-ion confinement and plasma performance. Losses of energetic alpha particles from DT fusion in ITER will reduce the alpha heating available to reach ignition, and have the potential to cause major damage to the first wall. Hence the behaviour of fast ions and their interaction with plasma instabilities in fusion plasmas has been extensively studied [1, 2], motivated by the fundamental importance of alpha particle heating in DT plasmas [3–5].

Energetic particle driven geodesic acoustic modes (EGAMs) occur early in the ramp-up of the plasma current in the DIII-D tokamak during counter neutral beam injection [6]. EGAMs are energetic particle modes with a mode frequency  $\sim 50\%$  below the ideal geodesic acoustic mode (GAM) frequency. A fluid-kinetic model [7] qualitatively replicates the observed mode characteristics, including rapid mode bursting and frequency chirping, and large electron density fluctuations without detectable electron temperature fluctuations. The nonperturbative electrostatic model shows the energetic particle pressure drives an  $n = 0$  radial electric field and a GAM-like  $m = 1$  density perturbation. The modes occur in plasmas with an elevated central safety factor ( $q_{\min} \geq 2$ ) and with comparable electron and ion temperatures, relevant to proposed steady-state plasma regimes [2]. Sharp drops ( $\sim 10\text{--}15\%$ ) in the neutron production are indicative of

strong beam ion redistribution and/or loss [6]. This paper concentrates on the observation of beam ion losses due to the EGAM mode activity.

A scintillator-based fast-ion loss detector (FILD) [8] has recently been installed on DIII-D (toroidal magnetic field = 2.1 T, major radius = 1.66 m, and minor radius = 0.67 m) to study energetic ion losses induced by Alfvén eigenmodes (AEs) and other MHD instabilities. Based on the design used on ASDEX Upgrade [9, 10], the light pattern resulting from ions striking a fast time response (decay time  $\sim 500$  ns) scintillator is imaged by a CCD camera, allowing measurements of the pitch angle and gyroradius of the beam ions reaching the detector. Light from the scintillator is also measured by a fibre-coupled photomultiplier to allow identification of AE and other high frequency instabilities. This paper reports the first experimental observations of beam ion losses in a tokamak due to EGAMs. The measured losses are compared to the results of a full orbit simulation code SPIRAL to better understand the beam ion transport resulting from interactions between the modes and confined ions. The EGAM-ion interaction occurs only in energy space, compared to the AE-ion interaction that involves the energy, canonical momentum, and magnetic moment of the ions. The EGAM-ion interaction is primarily electrostatic, with the  $n = 0$  nature of the EGAM leading to changes only in the ion energy (compared to AE-ion interactions that affect both ion energy and canonical momentum), thus providing a fundamental test of our ability to model the impact of MHD instabilities on energetic ions [11].

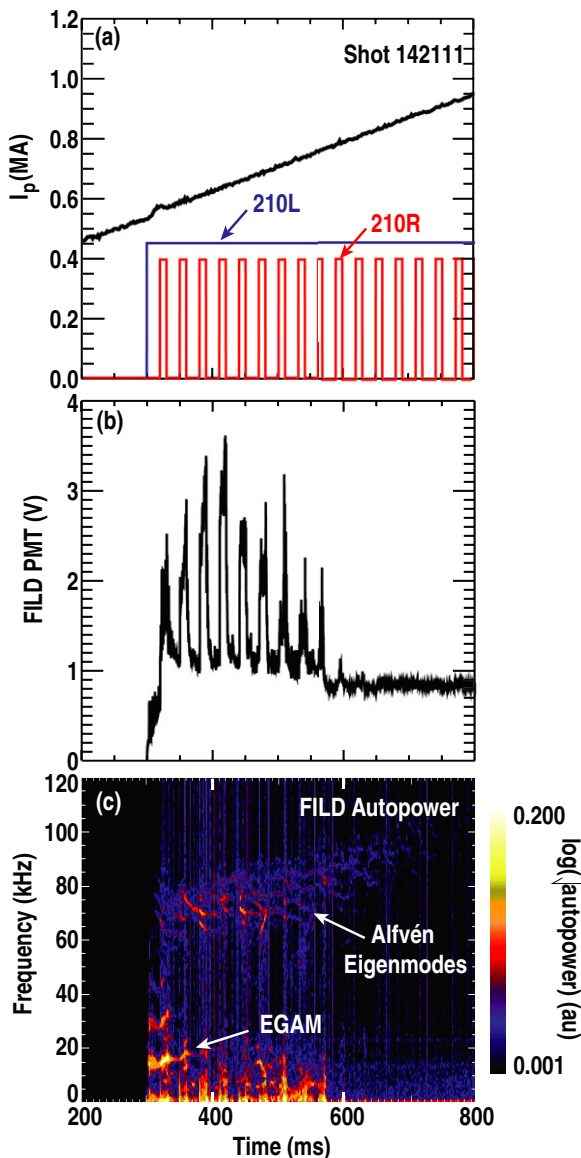


**Figure 1.** Time dependence of (a) neutral beam injection from 210R (shown in red and pulsed) and 210L (shown in blue and on continuously from 300 ms to 1000 ms) ion sources, (b) beam ion loss measured by FILD PMT and (c) time-resolved power spectrum of the beam ion loss signal showing strong EGAM activity at  $\sim 15$ – $45$  kHz occurring very early after the start of the beam injection.

## 2. Measured EGAM-induced beam ion losses

Neutral beam injection counter to the direction of the plasma current early in the ramp-up of the plasma current in DIII-D strongly excites EGAMs. Figure 1 is an example of a DIII-D discharge with significant AE and EGAM activity. Deuterium beams (labelled 210L and 210R) inject 75–81 keV neutrals in the toroidal direction opposite the plasma current and are the primary beams responsible for exciting the EGAMs. The 210L beam is injected more perpendicular to the toroidal magnetic field than the 210R beam [12]. Figure 1(a) shows that the 210L beam source is on continuously from 300 to 1000 ms, while the 210R source is pulsed for 10 ms on and 20 ms off, starting at 320 ms. Figure 1(b) shows the beam ion

loss signal measured by the FILD scintillator detector, while figure 1(c) shows the power spectrum of the fast-ion losses with toroidal Alfvén eigenmode (TAE), reverse shear Alfvén eigenmode (RSAE) and EGAM activity. The pulsed losses in phase with the 210R beam injection include both prompt losses and instability-induced losses. Orbit modelling shows that the prompt-loss contribution from the 210R beam reaches the FILD detector (located approximately  $45^\circ$  below the outer midplane) at lower values of the plasma current. As the plasma current increases, the energetic ion banana widths decrease, resulting in wall strike positions that are to the midplane and no longer detectable by the FILD (after  $\sim 600$  ms). The losses coherent with AE activity in the 50–100 kHz region [13, 14] fall as the plasma current increases since the AE activity becomes more core localized while the fast-ion loss boundaries are moving outward, reducing the ability of the AEs to place beam ions directly onto loss orbits. This paper concentrates on the EGAM activity between 15 and 45 kHz that dominates the losses very early (from 300 to 350 ms) in the discharge, when the energetic particle pressure is a significant fraction of the total plasma pressure. The low plasma current at this time results in an elevated  $q_{\min}$ , allowing the modes to arise without substantial thermal ion Landau damping and leading to a low fast-ion beta  $\beta_h$  threshold for the EGAM mode onset [6].

Figure 2 shows an expanded view of the 300–450 ms time period when the EGAM activity is largest. The time-resolved frequency analysis of an external magnetic pickup coil is shown in figure 2(a). Figure 2(b) shows that the EGAM amplitude measured by an external magnetic field pickup coil (blue trace), and the coherent component of the FILD measured beam ion loss signal (red trace). Both signals are calculated based on an  $\sim 2$  kHz band centred on the time-varying EGAM frequency. The coherent beam ion loss peaks shortly after beam injection starts at 300 ms, and then decays rapidly, while the mode amplitude indicated by the magnetic pickup coil decays more slowly. The coherent component of the FILD loss signal also clearly correlates with the pulsed time behaviour of the 210R beam source. The measured coherent loss shows both a ‘rapid’ signal that occurs in phase with the 210R beam injection, and a ‘delayed’ component that decays over several milliseconds after the 210R beam turns off. This decay time is far longer than the calculated  $< 100 \mu\text{s}$  transit time for ions kicked onto a direct loss orbit, indicating that the measured EGAM-induced losses are the result of resonances instead of a simple modulation of the neutral beam prompt loss. Once the 210R source turns off, the energy of the remaining confined beam ions decays on the classical slowing-down time scale. This reduces the number of beam ions capable of interacting with the EGAMs, and is thought to lead to the observed decay in the coherent loss signal after each 210R beam pulse. On a slower time scale, the increase in plasma current with time moves the loss boundary to higher energies where there are fewer beam ions to interact with the EGAMs. This effect, combined with the mode amplitude reduction, is qualitatively consistent with the drop in the observed coherent losses between 325 and 425 ms.

The bursting behaviour characteristic of EGAMs is clearly visible when the measured fast-ion loss signal is viewed on an expanded time scale, as shown in figure 3(a). The

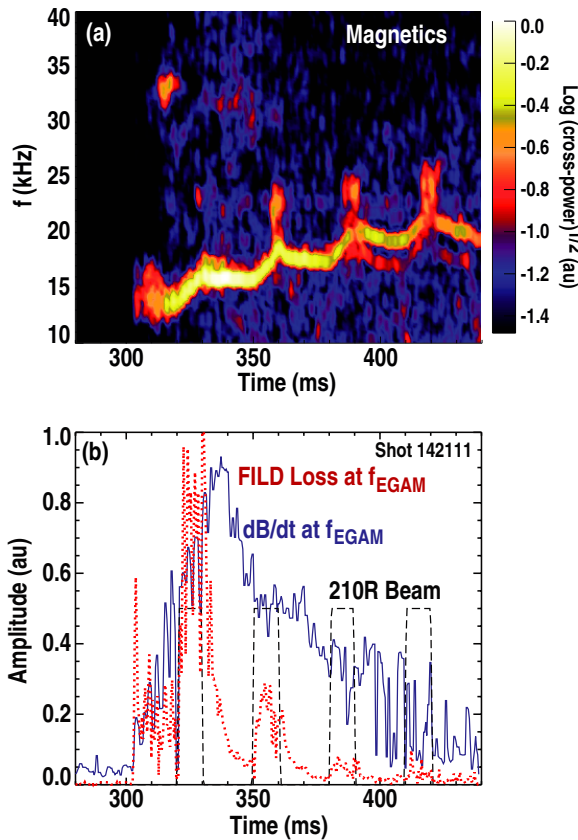


**Figure 2.** (a) Time-resolved power spectrum from an external magnetic pickup coil showing EGAM mode activity, and (b) time behaviour of the EGAM activity from the external magnetic pickup coil (blue trace) and the FILD measured beam ion loss (red trace). Both signals are the bandwidth filtered response in an  $\sim 2$  kHz band centred on the time-varying EGAM mode frequency. Also shown is the pulsed neutral beam injection from the 210R ion source (black trace).

coherent oscillations at the EGAM mode frequency  $\sim 15$  kHz are a significant fraction of the total loss signal. At 320 ms, the additional counter beam injection due to the 210R beam increases the measured losses. Figure 3(b) shows consecutive frames from the CCD camera imaging the light pattern created by beam ion losses striking the FILD scintillator plate. A grid indicating the gyroradius and pitch angle of the impacting ions is over plotted in white. The false colour images show significant losses occurring in two regions. The camera was operating at a frame rate of  $\sim 160$  frames  $s^{-1}$  and an exposure time of  $\sim 500$   $\mu s$  per frame. The frame taken at 325 ms shows a significant increase in the EGAM-induced losses (region circled in yellow in figures 3(b) and (c)) at pitch angles near  $45^\circ$ – $50^\circ$ . Analysis of the camera data shows that the EGAM losses build up during a 210R beam pulse and decay afterwards, consistent with the time behaviour of the PMT-measured coherent loss signal shown in figure 2.

The other region of losses, at pitch angles near  $\sim 70^\circ$  (region circled in red in figure 3(b)), does not change significantly between frames. Reverse orbit modelling shows that the losses near  $70^\circ$  are primarily due to prompt losses from the 210L beam, which is on continuously during this time period [14]. Prompt losses, or first orbit losses, result from ions born with orbits that intersect the outer wall. The

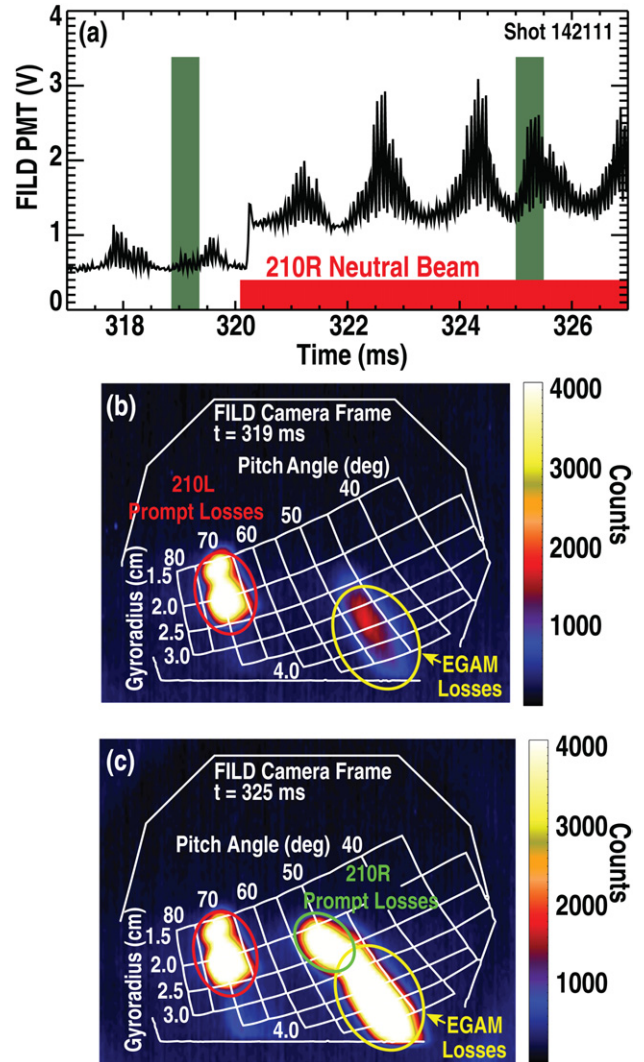


**Figure 3.** (a) Beam loss signal measured by FILD shows bursts of coherent ( $f \sim 15$  kHz) losses characteristic of EGAMs. The additional counter beam injection by the 210R source starting at 320 ms increases the measured loss rate. Consecutive frames at 319 ms (b) and 326 ms (c) from a CCD camera measuring the pitch angle and gyroradius of the losses show that the coherent losses appear at pitch angles near  $45^\circ$ – $50^\circ$ . The losses at pitch angles near  $70^\circ$  outlined in red do not change significantly and are predominantly due to prompt losses from the 210L source that is on continuously during this time period. The losses near  $45^\circ$ – $50^\circ$  in pitch angle are due to EGAM interactions (circled in yellow) and 210R prompt losses (circled in green).

losses near  $50^\circ$  in pitch angle are due to both first orbit (region circled in green in figure 3(b)) and EGAM-induced losses, and are primarily due to the 210R neutral beam source. These losses occur over a range of gyroradii from  $\sim 2$  to 4 cm. The magnetic field at the detector is 1.5 T, so this range of gyroradii corresponds to deuterium ion energies from  $\sim 25$  keV up to the maximum injected beam energy of  $E_b = 81$  keV. The 210L and 210R sources are the only neutral beams injecting counter to the direction of the plasma current in DIII-D (co-current beams provide another  $\sim 2$  MW of input heating in this shot), so the resulting beam ions are born on the inner leg of their banana orbits and it is not surprising that they dominate the observed loss signals.



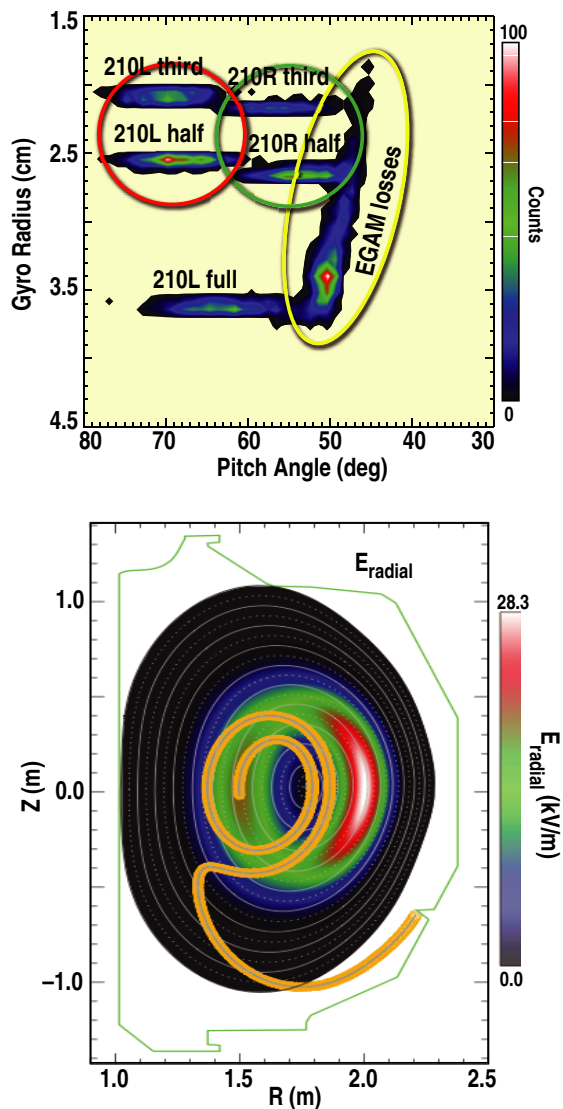


**Figure 4.** (a) Results of a full particle-orbit following code SPIRAL used to simulate the losses due to EGAMs are consistent with measured FILD results. (b) Calculated loss orbit (gold) for a beam ion detected in the EGAM-induced loss region of the FILD camera data ( $E = 75$  keV, pitch angle =  $45^\circ$ – $50^\circ$ ). Also shown is the calculated radial electric field from the  $m = 0$ ,  $n = 0$  electrostatic potential perturbation resulting from EGAM activity.

### 3. Modelling and inferred EGAM loss mechanism

SPIRAL is a full particle-orbit following code that was developed to model energetic ion behaviour in tokamaks [16, 17]. Figure 4 shows the results of SPIRAL used to simulate the losses due to EGAMs. In these SPIRAL code simulations<sup>1</sup>, ions with the birth energy deposition profile from NUBEAM [18] are followed as they slow down and pitch angle scatter while interacting with the  $m = 0$ ,  $n = 0$  radial electric field resulting from the EGAM activity. The radial electric field used in SPIRAL is calculated based on a toroidally symmetric electric potential which is a flux function, and whose magnitude is chosen to match the resulting density

<sup>1</sup> SPIRAL code was run on 512 AMD opteron processors using UNIX and followed 250000 particles (50000 per beam).

perturbation measured by a beam emission spectroscopy diagnostic. The EGAM-induced losses occur between  $45^\circ$  and  $50^\circ$  in pitch angle and over a broad range of gyroradii (regions circled in yellow in figures 4(a) and 3(b)) as the EGAMs interact with the slowing-down distribution of the 210R injected ions. Portions of the region near  $45^\circ$ – $50^\circ$  can also include prompt losses from the 210R source. An example is the region circled in green that is only present during 210R injection and is consistent with prompt losses for the one-third and one-half energy components of 210R. The SPIRAL results in figure 4 are in good agreement with the measured results in figure 3 and the same colour-coding is used to identify the different loss regions in both figures. Both the FILD measurements and the SPIRAL code predictions show significant EGAM-induced losses, comparable in magnitude to the prompt losses for the counter-injected beams. The SPIRAL results are also consistent with the measured time behaviour of the losses shown in figure 2, including the ‘delayed’ coherent component after the 210R beam is turned off.

Reverse orbit following techniques are used to calculate the orbits of the beam ions reaching the FILD detector based on their measured pitch angles and gyroradii. The magnetic field configuration inside the plasma is determined using the plasma equilibrium code EFIT [19], constrained by current profiles (based on motional Stark effect measurements of the magnetic field pitch) and the measured plasma pressure. Figure 4(b) shows the SPIRAL result for the poloidal projection of the calculated trajectory (shown in gold) for a 75 keV beam ion at a pitch angle of  $45^\circ$ – $50^\circ$  reaching the FILD detector. The inner portion of this unconfined trapped particle orbit is close to the orbits of confined counter-injected beam ions. As the counter-injected beam ions lose energy to the wave, the change in their pitch angle puts them on an unconfined trapped particle orbit, leading to the measured FILD loss signal coherent with the EGAM activity. Loss of the beam ions reduces the drive mechanism for the mode, which in turn reduces the beam loss rate until the cycle starts again. This predator–prey behaviour of the instability leads to the observed bursts in the mode amplitude and measured beam ion loss.

### 4. Conclusions

A new scintillator-based fast-ion loss detector on DIII-D has allowed the first experimental observations of fast-ion losses due to EGAM activity in a tokamak. Neutral beam injection counter to the direction of the plasma current strongly excites the EGAMs. From the measured pitch angle and gyroradii of the coherent beam ion loss signal, reverse orbit following techniques yield a trapped ion loss orbit with a large banana width that reaches well inside the plasma. Through the interaction with the EGAM, confined beam ions on counter-passing orbits experience a change in their pitch angle that places them on trapped particle loss orbits. The measured fast-ion loss exhibits the bursting behaviour characteristic of EGAMs, with a measured growth rate consistent with the fast-ion pressure driving the modes. The measured pitch angles and gyroradii of the measured fast-ion losses are consistent with the predictions of the full orbit following code SPIRAL used to model the EGAM-induced losses.

## Acknowledgments

This work was supported in part by the U.S. Department of Energy under DE-FC02-04ER 54698, SC-G903402 and DE-AC02-09CH11466. The assistance of the DIII-D team is gratefully acknowledged.

## References

- [1] Heidbrink W.W. and Sadler G.J. 1994 *Nucl. Fusion* **34** 535
- [2] Fasoli A. *et al* Progress in the ITER Physics Basis: chapter 5. Physics of energetic ions 2007 *Nucl. Fusion* **47** S264
- [3] Zweben S.J. 2000 *Nucl. Fusion* **40** 91
- [4] Heidbrink W.W. 2002 *Phys. Plasmas* **9** 2113
- [5] Keilhacker M. *et al* 1999 *Nucl. Fusion* **39** 209
- [6] Nazikian R. *et al* 2008 *Phys. Rev. Lett.* **101** 185001
- [7] Fu G.Y. *et al* 2008 *Phys. Rev. Lett.* **101** 185002
- [8] Fisher R.K. *et al* 2010 *Rev. Sci. Instrum.* **81** 10D307
- [9] García-Muñoz M. *et al* 2009 *Rev. Sci. Instrum.* **80** 053503
- [10] García-Muñoz M. *et al* 2010 *Phys. Rev. Lett.* **104** 185002
- [11] Berk H. *et al* 2006 *Nucl. Fusion* **46** S888
- [12] Heidbrink W.W. *et al* 2009 *Plasma Phys. Control. Fusion* **51** 125001
- [13] Pace D.C. *et al* 2011 *Plasma Phys. Control. Fusion* **53** 062001
- [14] Van Zeeland M.A. *et al* 2011 *Phys. Plasmas* **18** 056114
- [15] Pace D.C. *et al* 2010 *Rev. Sci. Instrum.* **81** 10D305
- [16] Kramer G.J. *et al* 2008 *Proc. 22nd Fusion Energy Conf. (Geneva, Switzerland)* (Vienna: IAEA) CCD-ROM le IT/P6-3 and [www.naweb.iaea.org/napc/physics/FEC/FEC2008/html/index.htm](http://www.naweb.iaea.org/napc/physics/FEC/FEC2008/html/index.htm)
- [17] Kramer G.J. *et al* 2012 A description of the full particle orbit following SPIRAL code for simulating fast-ion experiments in tokamaks *Plasma Phys. Control. Fusion* submitted
- [18] Pankin A. *et al* 2004 *Comput. Phys. Commun.* **159** 157
- [19] Lao L. *et al* 2005 *Fusion Sci. Technol.* **48** 968